Title	The importance of electron correlation on stacking interaction of adenine-thymine base-pair step in B-DNA: A quantum Monte Carlo study
Author(s)	Hongo, Kenta; Cuong, Nguyen Thanh; Maezono, Ryo
Citation	Journal of Chemical Theory and Computation, 9(2): 1081-1086
Issue Date	2013-01-09
Type	Journal Article
Text version	author
URL	http://hdl.handle.net/10119/16058
Rights	Kenta Hongo, Nguyen Thanh Cuong, and Ryo Maezono, Journal of Chemical Theory and Computation, 2013, 9(2), pp.1081-1086. This document is the unedited author's version of a Submitted Work that was subsequently accepted for publication in Journal of Chemical Theory and Computation, copyright (c) American Chemical Society after peer review To access the final edited and published work, see http://dx.doi.org/10.1021/ct301065f
Description	

The importance of electron correlation on stacking interaction of adenine-thymine base-pair step in B-DNA: A quantum Monte Carlo study

Kenta Hongo,[*],[†] Nguyen Thanh Cuong,[‡] and Ryo Maezono[†]

School of Information Science, JAIST, Asahidai 1-1, Nomi, Ishikawa 923-1292, Japan, and Nanosystem Research Institute (NRI), National Institute of Advanced Industrial Science and Technology (AIST), Tsukuba 305-8568, Japan

E-mail: kenta_hongo@mac.com

---

[*]To whom correspondence should be addressed

[†]School of Information Science, JAIST, Asahidai 1-1, Nomi, Ishikawa 923-1292, Japan

[‡]Nanosystem Research Institute (NRI), National Institute of Advanced Industrial Science and Technology (AIST), Tsukuba 305-8568, Japan

Abstract

We report fixed-node diffusion Monte Carlo (DMC) calculations of stacking interaction energy between two adenine(A)-thymine(T) base-pairs in B-DNA (AA:TT), for which reference data is available obtained from a complete basis set estimate of CCSD(T) (coupled-cluster with singles, doubles, and perturbative triples). We consider four set of nodal surfaces obtained from self-consistent field calculations, and examine how the different nodal surfaces affect the DMC potential energy curves of the AA:TT molecule and the resulting stacking energies. We find that the DMC potential energy curves using the different nodes look similar to each other as a whole. We also benchmark the performance of various QC methods, including Hartree-Fock (HF) theory, second-order Møller-Plesset perturbation theory (MP2), and density functional theory (DFT). The DMC and recently developed DFT results of the stacking energy reasonably agree with the reference, while the HF, MP2, and conventional DFT methods give unsatisfactory results.

KEYWORDS: Quantum Chemistry, Diffusion Monte Carlo, Density-Functional Theory, Dispersion.

Introduction

Noncovalent interactions are ubiquitous and play a fundamental role in biochemistry. It is widely recognized from a theoretical viewpoint that a major challenge in current quantum chemistry (QC) is to properly reproduce various types of noncovalent interactions in biomolecules.[1–5] Among them hydrogen (H-) bonding and stacking are of key importance. The H-bonding interaction can be described (more or less) qualitatively in terms of density functional theory (DFT) with conventional exchange-correlation (XC) functionals and even Hartree-Fock (HF) theory[2,3] because they can treat exchange repulsions and electrostatic forces. On the other hand, it is well known that both HF and standard DFT fail to describe the stacking interaction[4,5] due to their lack of dispersion interactions resulting from dynamical electron correlation effects at intermediate binding regions ("medium-range" electron correlation[6]). Hence a proper description of the stacking in

biomolecules requires higher levels of theory which capture the correlation effects.

DFT is the most commonly-used theoretical approach in QC because of its excellent balance between computational costs and accuracy.[7] Typical choices of approximate XC functionals are local density approximation (LDA),[8] generalized gradient approximation (GGA)[9–11] and its extension (meta-GGA),[12] and hybrid functionals.[13,14] Despite their success in applications to covalent systems, it has been shown that they are incapable of reproducing the dispersion interaction.[7] To overcome this pathology, numerous efforts have been made to develop new XC functionals: dispersion-corrected DFT (DFT-D),[15–18] a series of hybrid meta-GGA functionals developed by Truhlar and his coworkes,[19–21] long-range corrected DFT (LC-DFT),[22,23] DFT combined with symmetry-adapted perturbation theory (DFT-SAPT),[28] and so on. Although they usually agree reasonably well with experiments or high-level *ab initio* wave-function theory (WFT) methods,[7] it is hard to estimate their accuracy for new or untested systems. High-level treatment of the correlation based on WFT is needed as a reference for calibration to assess the performance of the functionals as well as to further develop new approximate DFT approaches.

Among correlated WFT approaches, second-order Møller-Plesset perturbation theory (MP2)[29] is the cheapest approximation to dynamical electron correlation at a computational cost of N^5, where N is the number of electrons in a system. It is well known, however, that MP2 generally tends to overbind dispersion interactions involving aromatic molecules (when large basis sets are employed).[30] This failure can be empirically improved by using MP2.5 or more general MP2.X,[31] though it involves a heavier computational cost. At present, coupled-cluster with single and double excitations including noniterative triples (CCSD(T))[29] is accepted to provide a more accurate intermolecular interactions, and hence is often called the "gold standard of QC". However, CCSD(T) is only applicable to small-sized noncovalent systems because it has a scaling behavior of N^7.

In the WFT approaches, an alternative is available for treating correlated wave functions, based on quantum Monte Carlo (QMC).[32,33] One of the most accurate and practical QMC methods is fixed-node diffusion Monte Carlo (DMC).[32,33] Within the constraint condition of a given fermion nodal hypersurface (fixed-node approximation), an imaginary-time evolution in DMC (stochastic

projection) usually yields a highly accurate energy comparable to CCSD(T). Furthermore, DMC has a more favorable scaling behavior of N^{3-4} with the system size[32,33], compared to CCSD(T), albeit with a large prefactor. This means that the DMC calculations are very CPU-time intensive. But recent advances in massively parallel computers mitigate this issue because of an ideal parallelizability of DMC.[34]

Thus DMC has been applied to some realistic noncovalent systems, and has successfully described their interactions.[35–41] In particular, Korth *et al.*[39] employed the S22 molecular set[42] for benchmarking the DMC performance. Their DMC results were in very good agreement with the best known reference values obtained from CCSD(T)/CBS (a complete basis set (CBS) estimate of CCSD(T)). Although the S22 set is well established for benchmarking *ab initio* approaches, it contains only simple biomolecular complexes, *e.g.*, the H-bonded Watson-Crick adenine(A)-thymine(T) base and dispersion-dominated A-T stacking pair. Although DMC has been applied to some noncovalent solids[40,41] due to its moderate computational cost, it has yet to be applied to larger and more complicated biomolecular systems.

In this paper we intend to benchmark the performance of DMC on describing more realistic noncovalent biomolecular systems. In particular, we examine effects of the fixed-node approximation in DMC. To this end, we chose as a benchmark system one of ten unique combinations of B-DNA base-pair steps, 5'-AA-3'//5'-TT-3' (hereafter abbreviated as AA:TT for simplicity). A reference data obtained from CCSD(T)/CBS with partitioning approximations[43] is available for the AA:TT stacking energy as well as its optimized molecular geometry, as shown in Fig. 1. In this study we focus on the vertical stacking interaction between the two Watson-Crick AT base pairs, which most significantly contributes to the stacking stability. We have performed DMC with several trial nodes to evaluate the stacking energies and potential curves, and then assessed their reliability, comparing with the reference data available. To plot the energy curve, we took interlayer distances of $2.7 - 10.0$ Å. In addition, we calibrate the performance of various QC approaches on their description of the AA:TT stacking interaction, comparing with the reference as well as our DMC results.
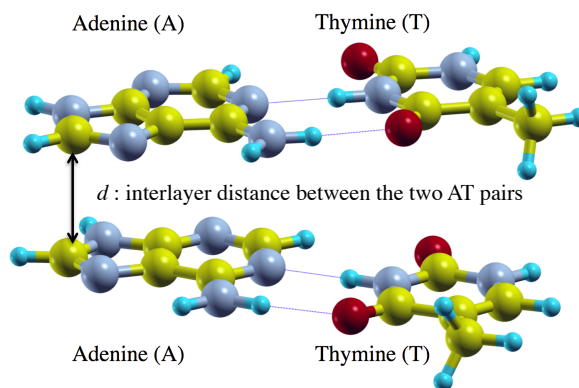
4

Figure 1: Molecular geometry of the 5'-AA-3'//5'-TT-3' (AA:TT) base pairs in B-DNA. An inter-layer distance (*d*) between the two hydrogen-bonded Watson-Crick adenine(A)-thymine(T) base pairs is variable, and all the other parameters are fixed as being the same as those in Ref.:[43] helical and propeller twist angles of 36° and 0°, respectively. The H, C, N, and O atoms are represented by sky blue, yellow, gray, and red colored balls, respectively.

Computational methods

Here we briefly describe our computational techniques for treating the target system. More detailed information about the standard theory is easily available in the literature.[32,33] In this study, all the QMC calculations were performed using the CASINO code,[32] while all the QC calculations were done using the Gaussian 09 code.[45]

For the C, N, and O atoms in the molecule, we replaced their two inner-core electrons (He core) with Burkatzki-Filippi-Dolg pseudopotentials (BFD-PPs).[44] The BFD-PP was also used for the H atom instead of its bare Coulomb interaction. As is common in DMC applications, Slater-Jastrow wave functions[32,33] were chosen as our trial nodes. The single-determinant parts were individually obtained from self-consistent field (SCF) calculations (HF or DFT). We considered the LDA (SVWN[8]), GGA (PBE[9]), and hybrid (B3LYP[11,13,14]) functionals for DFT. Hereafter we use the notation 'DMC/SCF' for DMC calculations with the SCF trial node. The one-body orbitals entering the determinant were expanded in terms of a VTZ basis set accompanied with the BFD-PPs.[44] We adopted a form of the Jastrow functions[46] implemented in the CASINO code,[47] including one-body, two-body (with the electron-electron cusps[48]), and three-body terms. Their

adjustable parameters were optimized by the variance minimization procedure.[49] Starting with the above trial nodes, DMC simulations were performed using random walkers with branching processes. In our DMC simulations, a target population of 1280 random walkers was used, and a time step was set to be 0.01 a.u., so that the time-step bias is less than chemical accuracy. To obtain converged results, we accumulated the numerical results over 10^5 steps after 500 equilibration steps. The T-move scheme[50] was used to evaluate the BFD-PP.

We also benchmark the performance of 18 functionals implemented in the Gaussian 09 code:[45] LDA (SVWN[8]); GGA (PBE,[9] PW91,[10] BLYP[11]); meta-GGA (TPSS[12]); hybrid (B3LYP;[11,13,14] PBE0;[24] mPW1PW91;[25] B97-1[26]); hybrid-meta-GGA (M05,[19] M05-2X,[20] M06,[21] M06-2X[21]); LC-DFT (CAM-B3LYP,[22] LC-ωPBE,[23] ωB97[27]); DFT-D (B97-D,[17] and ωB97X-D[18]). We considered WFT approaches including HF and MP2 as well. Although the BFD-PPs and the accompanying basis sets were developed for QMC, they can be used for other QC calculations as well.[44] We also examined the basis set dependence of potential energy curves (PECs), taking VTZ and VDZ with SVWN. We confirmed that the maximum energy deviation was enough small, 1.7 and 2.2 ± 1.8 kcal/mol for SVWN and DMC/SVWN, respectively. Thus all our QC calculations were performed using the BDF-PPs with the VTZ basis.

Results and Discussion

Potential energy curves

We now report our QC and DMC results of the potential energy curves (PECs) of the AA:TT molecule. Figure 2 shows the PECs obtained from (a) SCF (HF, SVWN, PBE, B3LYP) and MP2 calculations and (b) DMC with the four SCF trial nodes. For comparison CCSD(T)/CBS reference energies[43] at $d = 3.2$, 3.3, and 3.4 Å are also plotted in both the figures.

As shown in Fig. 2 (a), the AA:TT stacking interactions are not satisfactory described by the HF, GGA (PBE), and B3LYP calculations. This suggests that taking into account not only correlation itself but also a subtle balance of exchange and correlation is necessary for an appropriate de-
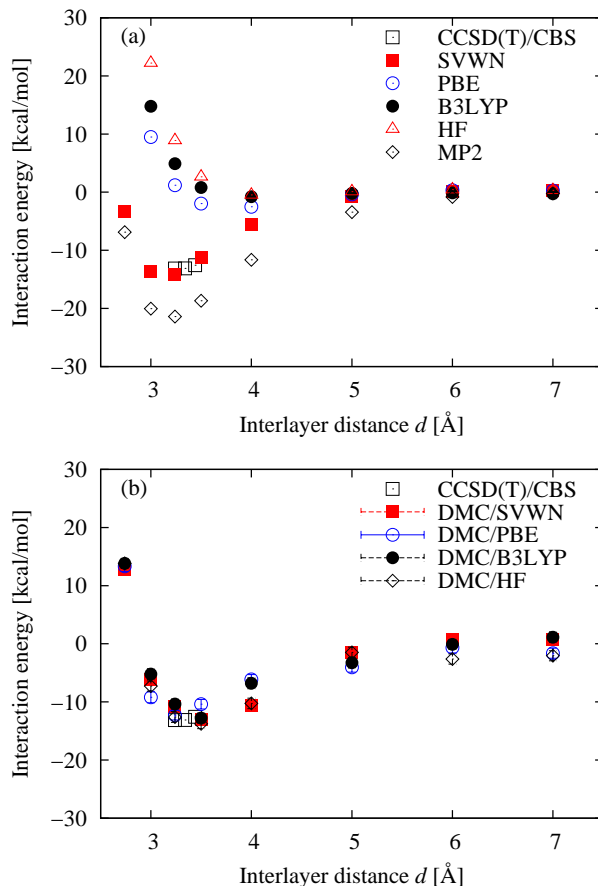
Figure 2: Potential energy curves obtained from various methods: (a) SCF (HF, DFT) and MP2 calculations and (b) DMC calculations with the SCF trial nodes. The energy at each d is shifted by the corresponding energy at $d = 10.0$ Å. In both the figures, CCSD(T)/CBS reference energies evaluated by Sponer *et al.*[43] are also shown for comparison.

scription of the stacking. In contrast, LDA reproduces the stacking, and its stacking energy (-14.1 kcal/mol at $d = 3.2$ Å) agrees with the CCSD(T)/CBS value (-13.1 kcal/mol at $d = 3.2$ Å),[43] even though LDA, by construction, cannot describe dispersion either. This artifact in LDA has been reported in some noncovalent systems, *e.g.*, graphitic systems.[51] By nature, MP2 describes the dynamical correlations, but overbinds significantly (-21.4 kcal/mol at $d = 3.2$ Å), compared to the CCSD(T)/CBS energy. It is well known that MP2 overestimates dispersion interactions involving aromatic groups when using large basis sets.[30]

On the other hand, we see from Fig. 2 (b) that the DMC PECs with the four different nodes (HF, SVWN, PBE, B3LYP) look similar to each other as a whole. The dependence of the DMC

7

PECs on the XC functionals is weakened by the DMC projection. This does not straightforwardly mean that the SCF nodes have a similar structure. In fact, a proper cancellation of fixed-node errors occurs between the stacked and separated systems, leading to the similarity in PECs between two DMC methods.
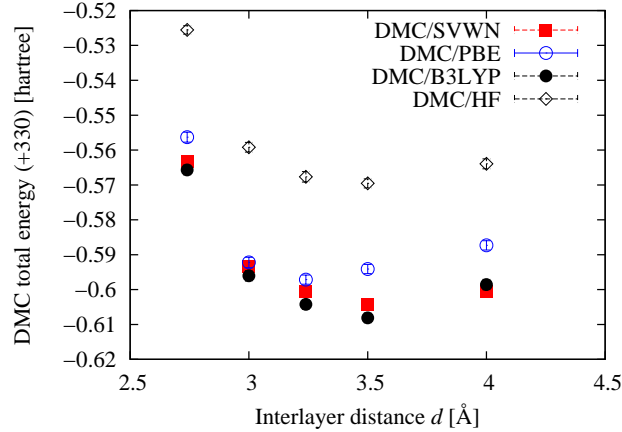

Figure 3: DMC total energy curves with the SCF trial nodes to see the fixed-node variational principles (see text). All the energies are shifted by $+330$ hartree.

To see in more detail how our trial nodes are different from each other, we plot the DMC total energies versus interlayer distances in Fig. 3. Note that the variational principle with respect to (fixed) trial nodes holds for the DMC total energy,[32,33] *i.e.*, trial nodes with lower energies are closer to the exact solution. We find that the HF node gives the highest energy, while the B3LYP does the lowest one; the difference between them is ~ 0.05 hartree. This trend has been also found for some transition-metal systems.[52,53]

It is found from Fig. 3 that the PBE node gives a shorter distance ($d \sim 3.2$ Å), while the other three nodes (HF, SVWN, and B3LYP) longer distances ($d \sim 3.5$ Å). These are reasonably good in agreement with the average distance observed in actual DNA structures ($3.3 \sim 3.4$ Å).[43] The DMC stacking energies around their equilibrium distances using the SVWN, PBE, B3LYP, and HF nodes were estimated to be -13.1 ± 0.9, -12.3 ± 0.9, -12.8 ± 0.9, and -13.8 ± 0.9 kcal/mol, respectively. They are also in reasonably good agreement with the reference value of -13.1 kcal/mol.[43] Overall the DMC projection gives a similar shape of the PECs, even starting

8

with the different trial nodes.
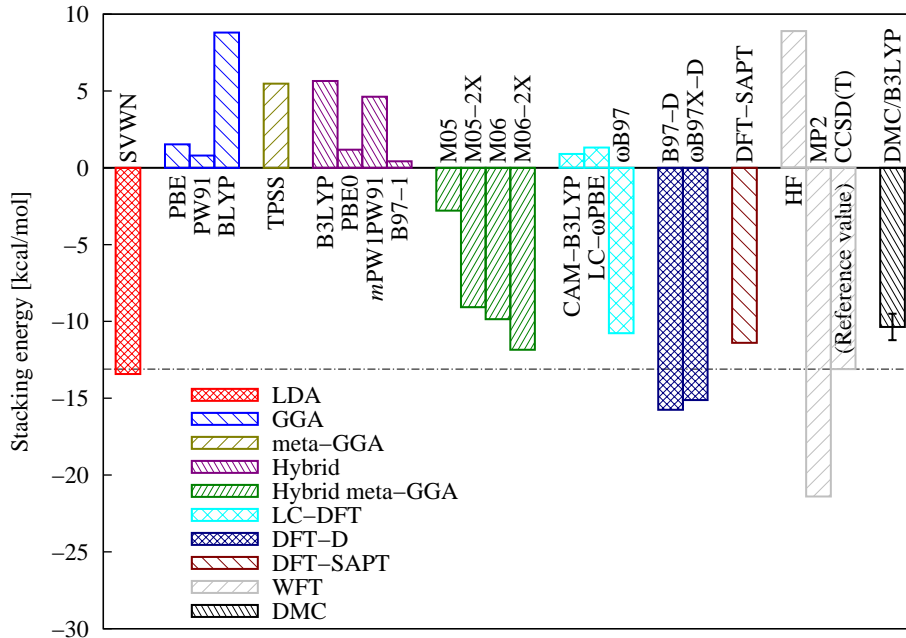
Benchmark of various methods

Figure 4: AA:TT stacking energies obtained from various methods (see text for the exact description of methods employed). A dashed line is drawn to hold the reference energy value at eye level.

Figure 4 summarizes the AA:TT stacking energies evaluated by various methods, compared with the reference energy value obtained from the CCSD(T)/CBS.[43] They were individually computed with a CCSD(T)/CBS-optimized geometry (fixed $d = 3.2$ Å)[43] except a DFT-SAPT result by Fiethen *et al.*[55] for comparative purpose. For DMC, we consider only the B3LYP node (DMC/B3LYP). Negative values of the stacking energy indicate that the dispersion is more or less captured, whereas positive values highlight challenges for describing the dispersion, or electron correlation. Apart from LDA, failures to reproduce the stacking (giving a positive sign) are found in all the conventional functionals including GGA, meta-GGA, hybrid functionals, all of which are appropriate for describing covalent systems. In contrast, most of the dispersion-corrected XC functionals were successful in capturing the stacking (giving a negative sign). In more detail, the

findings are as follows (numerical values of the stacking energies in units of kcal/mol are given in parentheses):

(1) The DFT-D methods, B97-D and ωB97X-D, give the correct sign, but slightly overbind (-15.8 and -15.1) compared to the reference value (-13.1). Although DFT-D methods usually show a good performance for most noncovalent systems, the overbinding in DFT-D has been reported in some cases.[54]

(2) The series of the hybrid-meta-GGA functionals, M05, M05-2X, M06, and M06-2X, successfully reproduces the stacking interaction, as expected. Among them M06-2X (-11.8) has the best agreement with the reference.

(3) The LC functional, ωB97, is found to predict the stacking properly (-10.8). Perhaps surprisingly, the other two LC functionals, CAM-B3LYP and LC-ωPBE, fail to give the correct sign. This implies that a proper treatment of "medium-range" correlation[6] is crucial. Furthermore, we find that when expanding upon three functionals, BLYP, B3LYP, and CAM-B3LYP, the more sophisticated treatment of the exchange term yields a better result. We suggest therefore that both the exchange and correlation should be taken into account in a balanced way.

As we mentioned before, HF completely fails to describe the stacking, whereas MP2 gives the correct sign, but significantly overbinds (-21.4). In contrast, DFT-SAPT gives a good result (-11.39),[55] compared to the reference. The DMC/B3LYP result (-10.4 ± 0.9) reasonably agrees with M06-2X, ωB97, and DFT-SAPT as well as the reference, though it is not the best variationally optimized value.

We note that the reference geometry employed in Fig. 4 is not necessarily optimum for the other methods (DMC, SCF, and MP2). For instance, the PBE functional gives an unbound state at the reference geometry, but it gives a shallow bound state (-2.5 kcal/mol) at a larger interlayer distance ($d = 4.0$ Å), as shown in Fig. 2 (a). In addition we note that Fig. 4 does not include BSSE (basis set superposition error) correction.[29] It is expected to correct the binding weaker and not to strongly depend on the choice of XC functionals. To estimate the magnitude we evaluated the BSSE energy using counterpoise methods[29] applied to LC-ωPBE and M06-2X. It is found from

10

Fig. 5 (a) that the counterpoise correction (CPC) gets the interaction weaker at every distance for both LC-ωPBE and M06-2X. The correction strongly depends on the interlayer distances, but not on the XC functionals employed, as shown in Fig. 5 (b); LC-ωPBE and M06-2X estimate the BSSE correction at the reference geometry to be 3.4 and 3.5 kcal/mol, respectively.
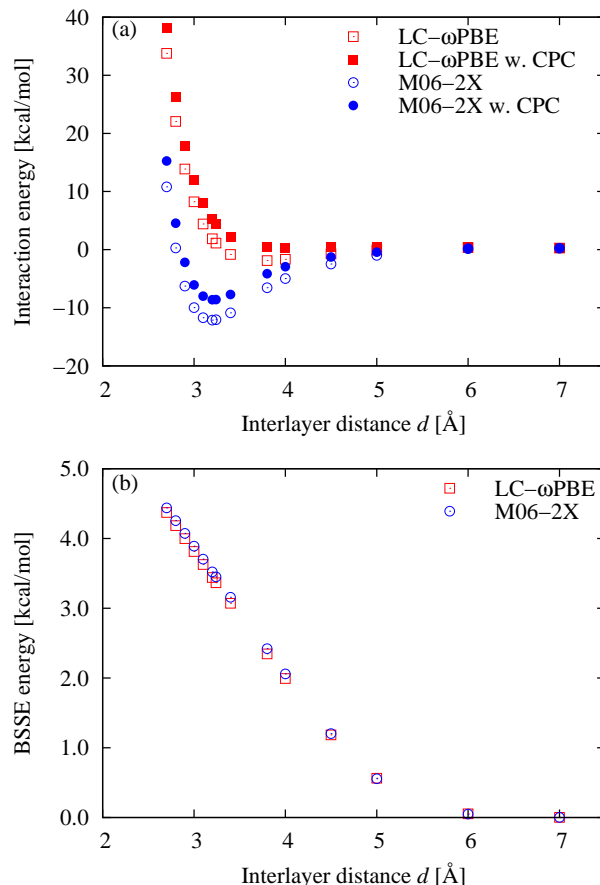

Figure 5: (a) Potential energy curves obtained from LC-ωPBE and M06-2X with or without the counterpoise correction (CPC). (b) BSSE energies obtained from LC-ωPBE and M06-2X.

Concluding remarks

In conclusion, we have applied DMC to the AA:TT molecule in order to calculate its stacking energy and potential energy curve (PEC). We explored the effect of different trial nodes (HF, LDA, GGA, and B3LYP) on the DMC evaluation of the PECs. It is found that the DMC projection

significantly reduces the node dependence, and the resulting PECs look similar to each other. In addition, we benchmarked various QC calculations based on DFT as well as WFT. In DFT, conventional semilocal and hybrid functionals fail to reproduce the stacking, whereas most of the recently developed functionals predict it properly, except for two LC functionals, indicating that a balanced inclusion of exchange and correlation is necessary for a proper description of the stacking. In WFT, HF and MP2 give unsatisfactory results, while DMC with the variationally best B3LYP node yields a stacking energy comparable to the CCSD(T)/CBS reference value.

Finally we shall remark computational issues. Our DMC calculations were feasible on our 32-core PC clusters. On the other hand, we attempted Grimme's double-hybrid functional (B2PLYP)[56] and CCSD(T) calculations using the VDZ basis set, but they won't run even on supercomputers (*e.g.*, SGI Altix UV1000). In comparison with such high-level QC approaches, DMC can be an alternative to give an accurate reference energy for medium to large-sized noncovalent systems to which high-level approaches are not generally applicable.

Acknowledgments

References

(1) Hobza, P.; Muller-Dethlefs, K. *Non-Covalent Interactions: Theory and Experiment*; Royal Society of Chemistry: Cambridge, UK, 2010.

(2) Hobza, P; Šponer, J. Structure, Energetic, and Dynamics of the Nucleic Acid Base Pairs: Nonempirical *Ab Initio* Calculations. *Chem. Rev.* **1999**, *99*, 3247-3276.

(3) Muller-Dethlefs, K.; Hobza, P. Noncovalent Interactions: A Challenge for Experiment and Theory. *Chem. Rev.* **2000**, *100*, 143-167.

(4) Černý, J.; Hobza, P. Non-covalent interactions in biomacromolecules. *Phys. Chem. Chem. Phys.* **2007**, *9*, 5291-5303.

(5) Riley, K. E.; Pitoňák, M.; Jurečka, P.; Hobza, P. Stabilization and Structure Calculations for Noncovalent Interactions in Extended Molecular Systems Based on Wave Function and Density Functional Theories. *Chem. Rev.* **2010**, *110*, 5023-5063.

(6) Zhao, Y.; Truhlar, D. G. Density Functionals for Noncovalent Interaction Energies of Biological Importance. *J. Chem. Theory Comput.* **2007**, *3*, 289-300.

(7) Cohen, A. J.; Mori-Sǎnchez, P. ; Yang, W. Challenges for Density Functional Theory. *Chem. Rev.* **2012**, *112*, 289-320.

(8) Vosko, S. H.; Wilk, L.; Nusair, M. Accurate spin-dependent electron liquid correlation energies for local spin density calculations: A critical analysis. *Can. J. Phys.* **1980**, *58*, 1200-1211.

(9) Perdew, J. P.; Burke, K.; Ernzerhof, M. Generalized gradient approximation made simple. *Phys. Rev. Lett.* **1996**, *77*, 3865-3868.

(10) Perdew, J. P.; Chevary, J. A.; Vosko, S. H.; Jackson, K. A.; Pederson, M. R.; Singh, D. J.; Fiolhais, C. Atoms, molecules, solids, and surfaces: Applications of the generalized gradient approximation for exchange and correlation. *Phys. Rev. B* **1992**, *46*, 6671-6687.

(11) Lee, C.; Yang, W.; Parr, R. G.; Development of the Colle-Salvetti Correlation-Energy Formula into a Functional of the Electron Density. *Phys. Rev. B* **1988**, *37*, 785-789.

(12) Tao, J. M.; Perdew, J. P.; Staroverov, V. N.; Scuseria, G. E. Climbing the Density Functional Ladder: Nonempirical Meta-Generalized Gradient Approximation Designed for Molecules and Solids. *Phys. Rev. Lett.* **2003**, *91*, 146401:1-4.

(13) Becke, A. D. Density-Functional Thermochemistry. III. The Role of Exact Exchange. *J.Chem.Phys.* **1993**, *98*, 5648-5652.

(14) Stephens, P. J.; Devlin, F. J.; Frisch, M. J.; Chabalowski, C. F. Ab Initio Calculation of Vibrational Absorption and Circular Dichroism Spectra Using Density Functional Force Fields. *J. Phys. Chem.* **1994**, *98*, 11623-11627.

(15) Grimme, S. Accurate Description of van der Waals Complexes by Density Functional Theory Including Empirical Corrections. *J. Comput. Chem.* **2004**, *25*, 1463-1473.

(16) Grimme, S.; Antony, J.; Ehrlich, S.; Krieg, H. A Consistent and Accurate *Ab Initio* Parametrization of Density Functional Dispersion Correction (DFT-D) for the 94 Elements H-Pu. *J. Chem. Phys.* **2010**, *132*, 154104:1-19.

(17) Grimme, S. Semiempirical GGA-Type Density Functional Constructed with a Long-Range Dispersion Correction. *J. Comp. Chem.* **2006**, *27*, 1787-1799.

(18) Chai, J.-D.; Head-Gordon, M.; Long-range Corrected Hybrid Density Functionals with Damped Atom-Atom Dispersion Corrections. *Phys. Chem. Chem. Phys.* **2008**, *10*, 6615-6620.

(19) Zhao, Y.; Schultz, N. E.; Truhlar, D. G.; Exchange-Correlation Functional with Broad Accuracy for Metallic and Nonmetallic Compounds, Kinetics, and Noncovalent Interactions. *J. Chem. Phys.* **2005**, *123*, 194101:1-18.

(20) Zhao, Y.; Schultz, N. E.; Truhlar, D. G. Design of Density Functionals by Combining the Method of Constraint Satisfaction with Parametrization for Thermochemistry, Thermochemical Kinetics, and Noncovalent Interactions. *J. Chem. Theory and Comput.* **2006**, *2*, 364-382.

(21) Zhao, Y.; Truhlar, D. G. The M06 Suite of Density Functionals for Main Group Thermochemistry, Thermochemical Kinetics, Noncovalent Interactions, Excited States, and Transition Elements: Two New Functionals and Systematic Testing of Four M06-Class Functionals and 12 Other Functionals. *Theor. Chem. Acc.* **2008**, *120*, 215-241.

(22) Yanai, T.; Tew, D.; Handy, N. A New Hybrid Exchange-Correlation Functional Using the Coulomb-Attenuating Method (CAM-B3LYP). *Chem. Phys. Lett.* **2004**, *393*, 51-57.

(23) Tawada, Y.; Tsuneda, T.; Yanagisawa, S.; Yanai, T.; Hirao, K. A Long-Range-Corrected Time-Dependent Density Functional Theory. *J. Chem. Phys.* **2004**, *120*, 8425-8433.

(24) Adamo, C.; Barone, V. Toward Reliable Density Functional Methods without Adjustable Parameters: The PBE0 model. *J. Chem. Phys.* **1999**, *110*, 6158-6169.

(25) Adamo, C.; Barone, V. Exchange Functionals with Improved Long-Range Behavior and Adiabatic Connection Methods without Adjustable Parameters: The mPW and mPW1PW Models. *J. Chem. Phys.* **1998**, *108*, 664-675.

(26) Hamprecht, F. A.; Cohen, A.; Tozer, D. J.; Handy, N. C. Development and Assessment of New Exchange-Correlation Functionals. *J. Chem. Phys.* **1998**, *109*, 6264-6271.

(27) Chai, J.-D.; Head-Gordon, M. Systematic Optimization of Long-Range Corrected Hybrid Density Functionals. *J. Chem. Phys.* **2008**, *128*, 084106.

(28) Hesselmann, A.; Jansen, G.; Schütz, M. Density-Functional Theory-Symmetry-Adapted Intermolecular Perturbation Theory with Density Fitting: A New Efficient Method to Study Intermolecular Energies. *J. Chem. Phys.* **2005**, *122*, 014103: 1-17.

(29) Helgaker, T.; Jørgensen, P.; Olsen, J. *Molecular Electronic-Structure Theory*, Wiley: Chichester, UK, 2000, .

(30) Riley, K. E.; Platts, J. A.; Řezáč, J.; Hobza, P.; Hill, J. G. Assessment of the Performance of MP2 and MP2 Variants for the Treatment of Noncovalent Interactions. *J. Phys. Chem. A* **2012**, *116*, 4159-4169.

(31) Riley, K. E.; Platts, J. A.; Řezáč, J.; Hobza, P. MP2.X: A Generalized MP2.5 Method that Produces Improved Binding Energies with Smaller Basis Sets. *Phys. Chem. Chem. Phys.* **2011**, *13*, 21121-21125.

(32) Needs, R. J.; Towler, M. D.; Drummond, N. D.; Lopez Rìos, P. Continuum Variational and Diffusion Quantum Monte Carlo Calculations. *J. Phys.: Condens. Matter* **2010**, *22*, 023201.

(33) Austin, B. M.; Zubarev, D. Y.; Lester, W. A. Jr. Quantum Monte Carlo and Related Approach. *Chem. Rev.* **2012**, *112*, 263-288.

(34) Gillan, M. J.; Towler, M. D.; Alfè, D. Petascale Computing Opens New Vistas for Quantum Monte Carlo. *Psi-k Highlight of the Month (Feburary 2011).*

(35) Benedek, N. A.; Snook, I. K.; Towler, M. D.; Needs, R. J. Quantum Monte Carlo Calculations of the Dissociation Energy of the Water Dimer. *J. Chem. Phys.* **2006**, *125*, 104302:1-5.

(36) Gurtubay, I. G.; Needs, R. J. Dissociation Energy of the Water Dimer from Quantum Monte Carlo Calculations. *J. Chem. Phys.* **2007**, *127*, 124306:1-8.

(37) Sorrela, S.; Casula, M.; Rocca, D. Weak Binding between Two Aromatic Rings: Feeling the van der Waals Attraction by Quantum Monte Carlo Methods. *J. Chem. Phys.* **2007**, *127*, 014105:1-12.

(38) Ma, J.; Alfè, D.; Michaelides, A.; Wang, E. The Water-Benzene Interaction: Insight from Electronic Structure Theories. *J. Chem. Phys.* **2009**, *130*, 154303:1-6.

(39) Korth, M.; Lüchow, A.; Grimme, S. Toward the Exact Solution of the Electronic Schrödinger Equation for Noncovalent Molecular Interactions: Worldwide Distributed Quantum Monte Carlo Calculations. *J. Phys. Chem. A* **2008**, *112*, 2104-2109.

(40) Drummond, N. D.; Needs, R. J. Quantum Monte Carlo, Density Functional Theory, and Pair Potential Studies of Solid Neon. *Phys. Rev. B* **2006**, **73**, 024107:1-8.

(41) Hongo, K.; Watson, W. A.; Sánchez-Carrera, R. S.; Iitaka, T.; Aspuru-Guzik, A. Failure of Conventional Density Functionals for the Prediction of Molecular Crystal Polymorphism: A Quantum Monte Carlo Study. *J. Phys. Chem. Lett.* **2010**, *1*, 1789-1794.

(42) Jurečka, P.; Šponer, J.; Černý, J.; Hobza, P. Benchmark Database of Accurate (MP2 and CCSD(T) Complet Basis Set Limit) Interaction Energies of Small Model Complexes, DNA Base Pairs, and Amino Acid Pairs. *Phys. Chem. Chem. Phys. 2006*, *8*, 1985-1993.

(43) Šponer, J.; Jurečka, P.; Marchan, I; Luque, F.J.; Orozeo, M.; Hobza, P. Nature of Base Staking: Reference Quantum-Chemical Stacking Energies in Ten Unique B-DNA Base-Pair Steps. *Chem. Eur. J.* **2006**, *12*, 2854-2865. A molecular geometry data employed in the present study can be downloaded from http://www.rsc.org/suppdata/CP/b6/b600027d/index.sht (accessed January 7, 2013).

(44) Burkatzki, M.; Filippi, C.; Dolg, M. Energy-Consistent Pseudopotentials for QMC calculations. *J. Chem. Phys.* **2007**, *126*, 234105:1-8. The present pseudopotentials and the accompanying Gaussian basis sets (VDZ and VTZ) are available from http://burkatzki.com/pseudos/impressum.2.html (accessed January 7, 2013).

(45) Frisch, M. J.; Trucks, G. W.; Schlegel, H. B.; Scuseria, G. E.; Robb, M. A.; Cheeseman, J. R.; Scalmani, G.; Barone, V.; Mennucci, B.; Petersson, G. A.; Nakatsuji, H.; Caricato, M.; Li, X.; Hratchian, H. P.; Izmaylov, A. F.; Bloino, J.; Zheng, G.; Sonnenberg, J. L.; Hada, M.; Ehara, M.; Toyota, K.; Fukuda, R.; Hasegawa, J.; Ishida, M.; Nakajima, T.; Honda, Y.; Kitao, O.; Nakai, H.; Vreven, T.; Montgomery, Jr., J. A.; Peralta, J. E.; Ogliaro, F.; Bearpark,

M.; Heyd, J. J.; Brothers, E.; Kudin, K. N.; Staroverov, V. N.; Kobayashi, R.; Normand, J.; Raghavachari, K.; Rendell, A.; Burant, J. C.; Iyengar, S. S.; Tomasi, J.; Cossi, M.; Rega, N.; Millam, J. M.; Klene, M.; Knox, J. E.; Cross, J. B.; Bakken, V.; Adamo, C.; Jaramillo, J.; Gomperts, R.; Stratmann, R. E.; Yazyev, O.; Austin, A. J.; Cammi, R.; Pomelli, C.; Ochterski, J. W.; Martin, R. L.; Morokuma, K.; Zakrzewski, V. G.; Voth, G. A.; Salvador, P.; Dannenberg, J. J.; Dapprich, S.; Daniels, A. D.; Farkas, O.; Foresman, J. B.; Ortiz, J. V.; Cioslowski, J.; Fox, D. J.: Gaussian 09, Revision A.1; Gaussian, Inc., Wallingford CT, 2009.

(46) Jastrow, R. J. Many-Body Problem with Strong Forces. *Phys. Rev.* **1955**, *98*, 1479-1484.

(47) Drummond, N.D.; Towler, M. D.; Needs, R. J. Jastrow Correlation Factor for Atoms, Molecules, and Solids. *Phys. Rev. B* **2004**, *70*, 235119:1-11.

(48) Kato, T.; On the Eigenfunctions of Many-Particle Systems in Quantum Mechanics. *Commun. Pure Appl. Math.* **1957**, *10*, 151-177.

(49) Drummond, N. D.; Needs, R. J.; Variance-Minimization Scheme for Optimizing Jastrow Factors. *Phys. Rev. B* **2005**, *72*, 085124:1-13.

(50) Casula, M. Beyond the Locality Approximation in the Standard Diffusion Monte Carlo. *Phys. Rev. B* **2006**, *74*, 161102(R):1-4.

(51) Hasegawa, M.; Nishidate, K. Semiempirical Approach to the Energetics of Interlayer Binding in Graphite. *Phys. Rev. B* **2004**, *70*, 205431:1-7.

(52) Kolorenč, J.; Hu, S.; Mitas, L. Wave Functions for Quantum Monte Carlo Calculations in Solids: Orbitals from Density Functional Theory with Hybrid Exchange-Correlation Functionals. *Phys. Rev. B* **2010**, *82*, 115108:1-8.

(53) Hongo, K.; Maezono, R. A Benchmark Quantum Monte Carlo Study of the Ground State Chromium. *Int. J. Quantum Chem.* **2011**, *112*, 1243-1255.

(54) Riley, K. E.; Pitoňák, M.; Černý, J.; Hobza, P. On the Structures and Geometry of Biomolecular Binding Motifs (Hydrogen-Bonding, Stacking, X-H$\cdots\pi$: WFT and DFT Calculations. *J. Chem. Theory Comput.* **2010**, *6*, 66-80.

(55) Fiethen, A.; Jansen, G.; Hesselmann, A.; Schütz, M. Stacking Energies for Average B-DNA Structures from the Combined Density Functional Theory and Symmetry-Adapted Perturbation Theory Approach. *J. Am. Chem. Soc.* **2008**, *130*, 1802-1803.

(56) Grimme, S. Semiempirical Hybrid Density Functional with Perturbative Second-Order Correlation. *J. Chem. Phys.* **2006**, *124*, 034108:1-16.

Graphical TOC Entry

The importance of electron correlation on stacking interaction of adenine:thymine base-pair step in B-DNA: A quantum Monte Carlo study